Molecular Photodetachment Microscopy

Christian Delsart, Fabienne Goldfarb, and Christophe Blondel*

Laboratoire Aimé-Cotton, Centre National de la Recherche Scientifique, Bâtiment 505, F-91405 Orsay Cedex, France†

(Received 5 July 2002; published 15 October 2002)

The photodetachment microscopy technique, which was originally used with atomic negative ions, is now applied to a molecular anion. The interferograms of several rotational thresholds corresponding to transitions from OH^- $X\,^1\Sigma^+$ $v = 0$ states to OH $X\,^2\Pi_{3/2,1/2}$ $v = 0$ states have been recorded. No effect due to the $1/r^2$ dipolar potential of the neutral molecule appears. Using a double-pass scheme of the laser on the negative ion beam, we measure the energy of the first few detachment thresholds with improved accuracy. The new recommended value of the electron affinity of ^{16}OH is 14 740.996(13) cm^{-1}, or 1.827 650 3(17) eV.

DOI: 10.1103/PhysRevLett.89.183002 PACS numbers: 33.80.Eh, 03.75.-b, 33.15.Ry, 33.60.-q

After having first offered direct views of an atomic electron wave function, photodetachment microscopy of negative ions has now established itself as a very sensitive technique for high accuracy measurements of the electron affinities of atoms [1,2]. As explained in the original Letters [3,4], photodetachment microscopy consists in directly imaging the spatial distribution of electrons photodetached from a negative ion in the presence of a uniform electric field. If the electric field is small compared to the internal fields of the atom (which is the usual laboratory situation), the electron comes out of the ion in the form of a spherical wave of energy ϵ, which is then folded back onto itself by the external field. The two halves of the wave interfere to produce a pattern cylindrically symmetric around the electric field direction.

The photodetachment images obtained in this way are actually very simple, for there is nearly no interaction of the outgoing electron with the neutral atomic core, except for a very weak induced-dipole $1/r^4$ potential. Photoionization, on the other hand, appears as another extreme, for the outgoing electron interacts with a positively charged core, i.e., via an infinite range $1/r$ Coulomb potential. As a consequence, photoionization microscopy involves classical trajectories [5] and quantum features [6] that appear much more complicated than in the photodetachment case; observation of the first photoionization microscopy images was reported only very recently [7].

Molecular anions offer us an intermediate case. If the neutral molecular core has a nonzero permanent electric dipole, the interaction of the excited electron has a $1/r^2$ asymptotic form. In this case, calculations have shown that the rescattering of one-half of the electron wave by the core may have detectable effects in the electron interferograms [8]. A special feature of the molecular case is the anisotropy of the $1/r^2$ potential created by the molecular dipole, which made the experiment all the more necessary in order to know whether detachment interferograms would still be observable, and how they would depend on the final rotation state.

Molecules, contrary to atoms, can also vibrate and rotate. The corresponding series of excitation energies become series of detachment thresholds, when one studies the photoexcitation of a molecular anion. This can be a severe drawback for photodetachment microscopy. A monoenergetic electron interferogram can be fitted to a 1 μeV accuracy, but the mix of images of different energies is more difficult to resolve. Only when photoelectron energies are more than 10 μeV apart does the disentanglement of interferograms become possible.

For the first attempt of molecular photodetachment microscopy, it was thus natural to look for a molecule with large rotational and vibrational spacings. Since the vibrational and rotational quanta scale as the square root of the inverse reduced mass of the nuclei and as the inverse moment of inertia of the molecule, respectively, hydrides are the best candidates. Among such ions, OH^- has been repeatedly used for studying the behavior of photodetachment cross sections in the vicinity of detachment thresholds, both theoretically [9,10] and experimentally [11,12] during the past 20 years.

Those detachment studies provide us with a rather complete background for the molecules involved in an $OH^- + h\nu \rightarrow OH + e^-$ experiment. A scheme of the first energy levels of both OH^- and OH, relevant for low-energy photodetachment studies, is given by Fig. 1.

The OH radical is one simple example of a diatomic molecule with a nonzero Λ orbital angular momentum in its electronic ground state. Ground state OH has a $\Lambda = 1$ total orbital angular momentum with total spin $S = 1/2$, i.e., a $^2\Pi$ term. Fine structure coupling makes the electronic energy of the molecule dependent on the sum of orbital and spin angular momenta, the projection of which on the internuclear axis can be either $\Omega = 3/2$, which has the lower energy, or $\Omega = 1/2$.

The vibrational quantum of energy of OH is so large (with a frequency higher than 100 THz) that we shall not consider any vibrational excitation. With J the rotation quantum number and I the moment of inertia of the molecule, rotation contributes a $\frac{J(J+1)\hbar^2}{2I}$ term to the total energy. In such a light molecule, the spin-orbit coupling is small enough to be overcome by the electron-rotation coupling as the rotational quantum number increases.

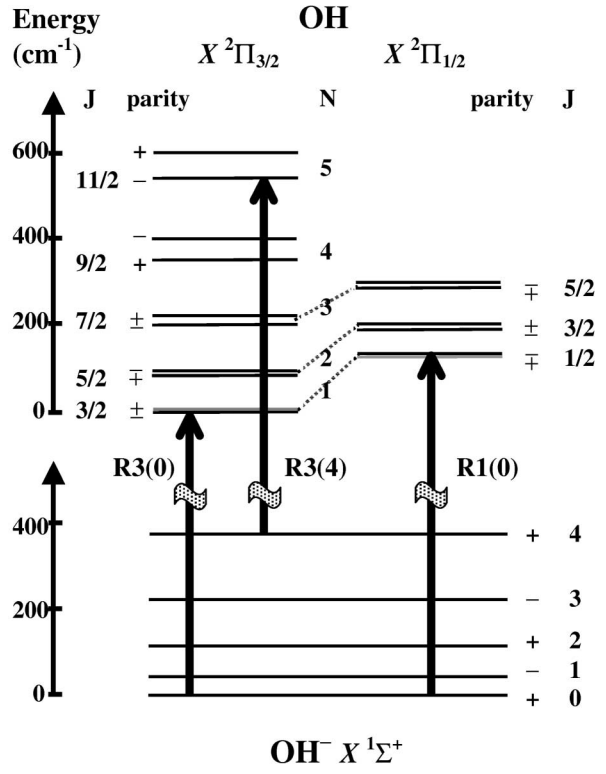

FIG. 1. The energy levels of OH^- and OH, for the first rotational states, both with zero vibrational quantum number. The Λ-doubling splittings have been exaggerated by a factor of 50 in order to be discerned.

Whereas for the slowly or nonrotating molecule Ω could be considered as a good quantum number [which, as a coupling case, is called Hund's case (a)], for higher rotation states a better characterization of the angular momentum states can be given by the value of N, the quantum number that results from coupling the electron orbital momentum Λ with the molecular rotation, without spin [Hund's case (b)].

Detachment transitions are labeled P, Q, R for a change of the N value by -1, 0, $+1$, respectively. Since even in Hund's case (b) the degeneracy of states with a given N value is partially removed by the fine structure, a digit 3 or 1 is added after the P, Q, or R label according to the original $\Omega = 3/2$ or $\Omega = 1/2$ character of the series. For instance, $R3(0)$ corresponds to detachment from an $N = 0$ state to a state of the series starting on $J = 3/2$, with an N variation of $+1$. This is the transition that defines the detachment energy, or electron affinity of OH.

Coupling the electron orbital momentum with the molecular rotation finally comes in to introduce a slight energy correction according to the levels' parity. If one thinks of the molecular rotation classically as defining a rotation plane (which necessarily contains the internuclear axis), the $\Lambda = 1$ electron orbital can extend either parallel or orthogonal to this plane, which makes it either possible or impossible to get mixed with the first excited electronic series $A\,^2\Sigma^+$. This cause of degeneracy removal, which makes the two possible orientations of the Π orbital directly visible on the energy spectrum, is called Λ doubling [13].

The lowest energy levels of the OH molecule, including the first vibrational states, are very well known; molecular parameters have been fitted to hundreds of lines and wave numbers have been tabulated to within 10^{-3} cm^{-1} [14].

As for the OH^- anion, closed electronic shells make its ground term a simpler $^1\Sigma^+$ one. The rotational constants of the $v = 0$ ground state of OH^- have been determined first by direct velocity modulation laser spectroscopy in a discharge cell [15] and, more recently, through the analysis of the high-resolution photodetachment spectra [12].

Experimental setup.—The experimental setup is the same as previously used for the study of atomic anions [2]. OH^- molecular anions are produced in a hot cathode discharge source fed with a stoichiometric mixture of N_2O and NH_3, completed with argon (respectively, 50%, 17%, and 33% of the mixture). Setting the ion source to a -1200 V potential provides the acceleration to the ion beam, which is calibrated to mass 17 by a Wien velocity filter (i.e., orthogonal electric and magnetic fields). Electrostatic optics help to collimate the beam and reduce its kinetic energy down to 500 eV. We obtain a beam of a few hundred pA in the interaction region.

The negative ions are detached in the presence of a uniform electric field of a few hundred $V\,m^{-1}$. The electron made free goes up along the electric field on a 0.514 m distance before being detected. The detector [16] is composed by microchannel plates (MCPs) followed by a surface-resistive anode, which detects the mean position of the electron bunch produced by the MCPs after each electron arrival. Such a detection scheme supposes that detachment events always be delayed by microseconds with respect to one another, which is essentially true for low-power cw laser photodetachment.

Photoexcitation is provided by a single mode cw dye laser (Spectra-Physics 360 A) operated with 4-dicyanomethylene-2-methyl-6-p-dimethylaminostyryl-4-H-pyran (DCM) in a solvent made of ethylene-glycol and benzyl alcohol (2/5, 3/5). At the detachment wavelengths, which range between 670 and 680 nm, the power of the laser ranges between 100 and 150 mW. External locking on a static sigmameter [17] makes the frequency stability better than 10 MHz. The exact wavelength is measured by comparison with the one of a stabilized He-Ne laser [18].

The photon energy is modified by the Doppler effect, which can be measured by making the laser intersect the ion beam twice, forth and back, on different locations. Two electron images are obtained, with symmetrical Doppler shifts. Energy ϵ that would have resulted from Doppler-free excitation is obtained by averaging the output energies of the two spots [1,2].

Results.—Experiments have been performed at the $R3(0)$, $R1(0)$, and $R3(4)$ thresholds. The $R3(4)$ case was chosen in order to test the feasibility of the experiment

with a significantly high value of the rotational quantum number. The question was whether an electron interference pattern would still be visible, as with atomic anions, and whether the isotropy and radial distribution of detection probability would still obey the atomic formula.

Figure 2 shows an image recorded in the $R3(0)$ case. Interference ring patterns are clearly visible. Isotropy of their intensity is consistent with the emission of an s wave (i.e., a free-electron the orbital angular momentum ℓ of which is zero), as expected by electric-dipole excitation of a π electron. The d wave ($\ell = 2$), though also allowed, does not appear, due to the very low excitation energy above threshold that makes it unlikely for the electron to overcome the centrifugal barrier.

The quantitative analysis of the images relies on the high sensitivity of the pattern to the initial kinetic energy ϵ of the electron. In atomic photodetachment microscopy experiments, very good results have been obtained by fitting the images with the model of a free-electron emitted from a pointlike source, i.e., the (squared) Green function of the uniform acceleration problem [19,20]. Using the same form for a quantitative analysis of the OH^- interference patterns, we obtain an agreement between theory and experiments that tends to indicate the absence of any detectable perturbations due to the molecular dipole. This makes it possible to measure ϵ with a high precision. Subtracting it from the photon energy, one obtains an estimate of the detachment threshold.

Uncertainty, in our threshold measurements, comes from the statistical dispersion of the fits and of the laser wavelength measurements, and possible systematic errors on the field value, the distance between detachment zones and the kinetic energy of the ion beam. All sources of uncertainties must be added together if one wants a complete confidence interval on the detachment energies. Making threshold differences has the advantage of eliminating the unknown systematic errors, and provides a test of molecular spectroscopic data, as shown by Table I. The difference between $R1(0)$ and $R3(0)$ agrees with the value of the fine structure given by Coxon [14]. If we rely on Coxon for higher energy intervals in OH, we find that the difference between $R3(0)$ and $R3(4)$ fits exactly with the value calculated after the data of Rosenbaum *et al.* for the OH^- molecule [15], but is lower than the estimation made after the rotational constants of Smith *et al.* by 89 mk [12].

The spectroscopic uncertainties on the internal structure of OH and OH^- are $\pm 10^{-3}$ and $\pm 3 \times 10^{-3}$ cm^{-1}, respectively. Taking them into account, we can have the photodetachment microscopy determined $R1(0)$ and $R3(4)$ thresholds contribute to a global estimate of the electron affinity of OH, which is directly measured by the $R3(0)$ threshold to be 14 740.991(19) cm^{-1}. The resulting value of the electron affinity is 14 740.990(15) cm^{-1}, which remains compatible with the previous measurement of 14 741.02(3) cm^{-1} [12] but lowers the most probable value by 0.030 cm^{-1}. Combination of the two could lead to a recommended value of 14 740.996(13) cm^{-1}, i.e., 1.827 650 3(17) eV. The last calculated value of 1.828 eV [21] agrees to three decimal places with this result.

Studies of the behavior of the photodetachment signal from OH^- as a function of the energy are always done, either theoretically [9,10] or experimentally [11,12], with reference to the universal power laws that cross sections are supposed to follow near thresholds [22]. Numerous experiments with atomic anions have actually shown photodetachment cross sections that do obey the so-called "Wigner law," i.e., increase with the energy ϵ as $\epsilon^{\ell+1/2}$. When emission of an s-wave is allowed by the electric-dipole selection rule and favored by the centrifugal effect, the onset of detachment appears conspicuously as a sudden increase of the photodetachment cross section, proportional to $\sqrt{\epsilon}$.

In all discussions about whether OH^- detachment actually follows the Wigner law, the ratio of the time it takes for the electron to leave the molecule to the rotational period appears as an essential parameter. In heavy molecules, rotation is slow compared to the outer electron motion, and the only problem is to describe the transition from a Born-Oppenheimer situation at short distances to a situation, at large distances, where the electron motion decouples from the molecular rotation [23,24]. The

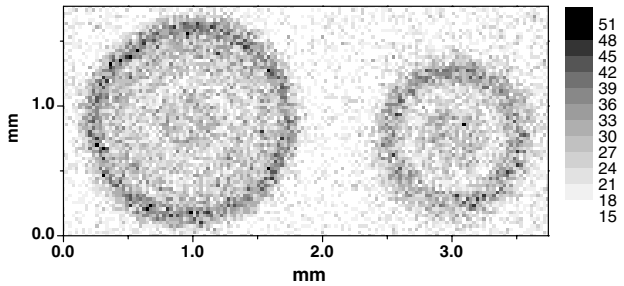

FIG. 2. A photodetachment double spot recorded within a 301 $V\,m^{-1}$ electric field just above the $R3(0)$ threshold of $^{16}OH^-$. The laser wavelength was 678 352.6 pm (vacuum). The left-hand and right-hand spots are produced by electrons, the emission kinetic energy of which was 0.792 and 0.430 cm^{-1}, respectively. The scale gives the number of electrons detected per pixel.

TABLE I. Threshold intervals (cm^{-1}), which eliminate the electron affinity unknown, are shown here as tests of the spectroscopic data on OH and OH^-.

Difference	Expected	Expected	This work
$R1(0)$–$R3(0)$	126.453[a]		126.451(21)
$R3(4)$–$R3(0)$	169.685[b]	169.776[c]	169.687(26)

[a]According to Coxon [14].
[b]According to Coxon [14] and Rosenbaum *et al.* [15].
[c]According to Coxon [14] and Smith *et al.* [12].

present situation however, is that of a particularly slow electron leaving from a molecule with an extremely large rotation constant, which, by comparison, makes the electron motion slow with respect to molecular rotation [25] even in the initial stage of the detachment process. As a consequence, one can expect the electric-dipole to be washed out by molecular rotation, for low-energy electrons, in all cases where the angular momentum of the neutral molecule is entirely due to nuclear motion [9].

The OH molecule, in this respect, has the advantage of having an internal electronic momentum (Π state), which makes it possible for the total angular momentum to have a nonzero component parallel to the internuclear axis. This can prevent rotation from averaging the dipole down to zero. Yet the additional Λ-doubling effect removes the degeneracy between states of different parities, which makes the unperturbed molecular levels states of zero electric dipole [10]. Only in the case of low experimental resolution, where Λ doublets are unresolved, do non-Wigner power laws appear at detachment thresholds [12].

At higher resolutions, the behavior of the cross section depends on whether the parity-favored channel is the lower or the upper threshold of the Λ doublet. In the former case, the lowest energy values actually correspond to a well-defined parity of the residual molecule, hence, with no electric-dipole influence, and the usual $\epsilon^{1/2}$ power law is observed [11]. The static field present in our experiment does not mix the Λ-doublet states in an appreciable way (several 10^4 V m^{-1} are needed, see [26]). Correspondingly, the images obtained in the $R3(0)$ and $R3(4)$ cases appear interaction free.

The second case appears more complicated [10], with no power law valid for the p wave emitted between the two thresholds and an increase of the cross section sharper than the normal $\epsilon^{1/2}$ law even at high energy resolution above the upper threshold [12]. The key effect is the high polarizability of the molecule by the outgoing electron. Yet orders of magnitude suggest that significant polarization takes place only in the first few tens of nm of its flight, while the phase of the interferogram builds up along several μm of the electron wave expansion. The influence of the induced dipole on the outgoing electron wave may thus remain negligible, which could explain the unperturbed character of our $R1(0)$ images also.

Conclusion.—Photodetachment microscopy forming a polar molecule has been performed and shown to produce electron interferograms that can be fitted as easily with the free-electron model as those obtained from atomic anions. Further investigation is needed to determine what the role of the Λ doubling can be, in relation to its observed influence on the cross-section variation at thresholds, for such an invariance. Rotational averaging might be avoided by bringing the molecule to well-chosen rotational sublevels, which could be achieved by using proper laser polarizations or multiphoton excitation. Lower energy-to-field ratios should be aimed at, anyway, in order to bring rescattering effects to observation, for the probability for such effects varies as $(F/\epsilon)^2$. The maintained agreement of the experimental results with the standard theory of photodetachment microscopy made it possible to get an improved measurement of the electron affinity of a molecule. The method will thus be applied profitably to other molecular anions.

The authors gratefully acknowledge instructive discussions with Christian Jungen and Maurice Raoult.

*Electronic address: christophe.blondel@lac.u-psud.fr
†URL: http://www.lac.u-psud.fr

[1] C. Blondel, C. Delsart, and F. Goldfarb, J. Phys. B **34**, L281 (2001); **34**, 2757 (2001).
[2] C. Blondel, C. Delsart, C. Valli, S. Yiou, M. Godefroid, and S. V. Eck, Phys. Rev. A **64**, 052504 (2001).
[3] Y. N. Demkov, V. D. Kondratovich, and V. N. Ostrovskii, Pis'ma Zh. Eksp. Teor. Fiz. **34**, 425 (1981) [JETP Lett. **34**, 403 (1981)].
[4] C. Blondel, C. Delsart, and F. Dulieu, Phys. Rev. Lett. **77**, 3755 (1996).
[5] C. Bordas, Phys. Rev. A **58**, 400 (1998).
[6] C. Nicole, I. Sluimer, F. Rosca-Pruna, M. Warntjes, M. Vrakking, C. Bordas, F. Texier, and F. Robicheaux, Phys. Rev. Lett. **85**, 4024 (2000).
[7] C. Nicole, H. L. Offerhaus, M. J. J. Vrakking, F. Lépine, and C. Bordas, Phys. Rev. Lett. **88**, 133001 (2002).
[8] I. I. Fabrikant (private communication).
[9] P. C. Engelking, Phys. Rev. A **26**, 740 (1982).
[10] P. C. Engelking and D. R. Herrick, Phys. Rev. A **29**, 2425 (1984).
[11] P. A. Schulz, R. D. Mead, P. L. Jones, and W. C. Lineberger, J. Chem. Phys. **77**, 1153 (1982).
[12] J. R. Smith, J. B. Kim, and W. C. Lineberger, Phys. Rev. A **55**, 2036 (1997).
[13] R. S. Mulliken and A. Christy, Phys. Rev. **38**, 87 (1931).
[14] J. A. Coxon, Can. J. Phys. **58**, 933 (1980).
[15] N. H. Rosenbaum, J. C. Owrutsky, L. M. Tack, and R. J. Saykally, J. Chem. Phys. **84**, 5308 (1986).
[16] Model 3391 of Quantar Technology Inc., 200 Washington Street 101, Santa Cruz, CA 95060-4976.
[17] P. Juncar and J. Pinard, Opt. Commun. **14**, 438 (1975).
[18] J. L. Hall and S. A. Lee, Appl. Phys. Lett. **29**, 367 (1976).
[19] V. D. Kondratovich and V. N. Ostrovsky, J. Phys. B **23**, 3785 (1990).
[20] C. Bracher, W. Becker, S. A. Gurvitz, M. Kleber, and M. S. Marinov, Am. J. Phys. **66**, 38 (1998).
[21] J. M. L. Martin, Spectrochim. Acta, Pt. A **57**, 875 (2001).
[22] E. P. Wigner, Phys. Rev. **73**, 1002 (1948).
[23] C. H. Greene and A. R. P. Rau, Phys. Rev. A **32**, 1352 (1985).
[24] D. C. Clary, J. Phys. Chem. **92**, 3173 (1988
[25] D. R. Herrick and P. C. Engelking, Phys. Rev. A **29**, 2421 (1984).
[26] K. I. Peterson, G. T. Fraser, and W. Klemperer, Can. J. Phys. **62**, 1502 (1984).